

See discussions, stats, and author profiles for this publication at: <https://www.researchgate.net/publication/263956947>

# Adsorption of Short-Chain Alcohols by Hydrophobic Silica Aerogels

ARTICLE in INDUSTRIAL & ENGINEERING CHEMISTRY RESEARCH · DECEMBER 2013

Impact Factor: 2.59 · DOI: 10.1021/ie4032023

---

READS

56

8 AUTHORS, INCLUDING:



Thomas J. Levario

Georgia Institute of Technology

6 PUBLICATIONS 31 CITATIONS

SEE PROFILE



Nick N. Linneen

Arizona State University

5 PUBLICATIONS 37 CITATIONS

SEE PROFILE



Robert Pfeffer

Arizona State University

177 PUBLICATIONS 4,803 CITATIONS

SEE PROFILE



Jerry Y S Lin

Arizona State University

307 PUBLICATIONS 9,535 CITATIONS

SEE PROFILE

# Adsorption of Short-Chain Alcohols by Hydrophobic Silica Aerogels

Michael Wiehn, Thomas J. Levorio, Kyle Staggs, Nick Linneen, Yuchen Wang, Robert Pfeffer, Y. S. Lin, and David R. Nielsen\*

School for Engineering of Matter, Transport, and Energy, Chemical Engineering Program, Arizona State University, 501 E. Tyler Mall, ECG 301, Tempe, Arizona 85287-6106, United States

**ABSTRACT:** The hydrophobic silica aerogel Cabot Nanogel TLD302 was evaluated as an adsorbent for recovering 2–5 carbon *n*-alcohols from aqueous solutions. Whereas intraparticle transport limitations restricted adsorption under dilute conditions, at higher concentrations, improved surface wetting resulted in facile “pore intrusion” and ~5-fold increases in adsorption capacity for all alcohols. To promote surface wetting and pore intrusion at lower concentrations, partial oxidation of TLD302 was performed by heat treatment to create a series of novel aerogel materials with tunable surface hydrophobicities. An optimum surface oxidation state was found to exist wherein pore intrusion under dilute conditions was achieved while still balancing high adsorption affinity. Lastly, the optimized aerogel adsorbent was used to recover *n*-butanol from a *Clostridium acetobutylicum* ATCC 824 fermentation broth. Relative to model solutions, no loss of adsorption affinity or capacity was observed, indicating that competitive coadsorption by other media components was not a performance-limiting factor.

## INTRODUCTION

Silica aerogels are sol–gel derived porous inorganic materials recognized for their low density (as low as 0.01–0.02 g/cm<sup>3</sup>),<sup>1</sup> high porosity (>90%),<sup>2</sup> and high specific surface area (600–1000 m<sup>2</sup>/g).<sup>3</sup> Aerogel surfaces are traditionally either hydrophilic or hydrophobic in nature, as determined by their surface chemistry and synthesis scheme. Whereas hydrophilic aerogels typically possess Si–OH surface functionality, the replacement of hydroxyl groups with hydrolytically stable hydrocarbon moieties renders their surfaces as hydrophobic.<sup>4</sup> Recently, hydrophobic aerogels have been investigated as adsorbents of aromatic wastewater contaminants (including toluene and xylenes)<sup>4–7</sup> as well as in the simulated cleanup of oil spills.<sup>3,8</sup> For example, hydrophobic methyltriethoxysilane<sup>9</sup> and tetraethoxysilane-derived<sup>10</sup> silica aerogels have been synthesized and found to serve as effective adsorbents for the uptake of nitrobenzene from wastewater.<sup>11</sup> In addition, –CH<sub>2</sub>CH<sub>2</sub>CF<sub>3</sub> surface-functionalized hydrophobic aerogels were effective at adsorbing hydrocarbon mixtures from simulated produced waters.<sup>12</sup>

Effective separation of lower alcohols from aqueous solutions is an important challenge, particularly with respect to sustainable biofuels production. In industry, ethanol and *n*-butanol are separated from aqueous fermentation broths via cost and energy intensive multistage distillation.<sup>13–15</sup> Several alternative strategies have been explored, however, including adsorption,<sup>16–20</sup> membrane pervaporation,<sup>21,22</sup> and gas stripping<sup>23,24</sup> (for a recent review see Vane<sup>25</sup>). Among these, it has been proposed that adsorption possesses the lowest energy demands,<sup>26,27</sup> and numerous materials have been proposed and characterized as adsorbent media, including polymer resins,<sup>16,26,28</sup> zeolites,<sup>18,20</sup> and activated carbon.<sup>19,26</sup> Irrespective of their nature, the most effective and highest capacity alcohol adsorbents are those possessing hydrophobic surface chemistries, to support stronger surface interactions through van der Waals forces,<sup>18</sup> and high specific surface areas.<sup>28</sup> As hydrophobic silica aerogels possesses both of these key attributes, it

was postulated that they might also serve as effective adsorbents for the separation of short-chain alcohols from aqueous solutions. Accordingly, the present study examined the adsorption performance and behavior of the trimethyl surface functionalized (i.e., Si–C(CH<sub>3</sub>)<sub>3</sub>), hydrophobic aerogel Cabot Nanogel TLD302 with respect to 2–5 carbon *n*-alcohols, including the biofuel alcohols ethanol and *n*-butanol. To the best of our knowledge, no prior studies have explored the use of hydrophobic aerogels as alcohol adsorbents.

## MATERIALS AND METHODS

**Chemicals.** Ethanol (95%, HPLC grade), *n*-propanol (99%, ACS grade), *n*-butanol (99.5%, reagent grade), and *n*-pentanol (98%, ACS grade) were each purchased from Fisher Scientific (Pittsburgh, PA).

**Silica Aerogels.** The hydrophobic silica aerogel Cabot Nanogel TLD302 (hereafter TLD302), whose relevant physical characteristics are summarized in Table 1, was supplied in particulate form by Cabot Corporation (Boston, MA) and nominally used as received with no pretreatment. Modification of TLD302's surface chemistry was performed via its partial to complete oxidation in a muffle furnace (Vulcan 3-550PD,

**Table 1. Relevant Characteristics of TLD302**

porosity <sup>a</sup>	95%
pore diameter (nm) <sup>a</sup>	20–40
particle diameter (mm) <sup>a</sup>	1.70–2.35
specific surface area (m <sup>2</sup> /g) <sup>a</sup>	~750
contact angle (degrees) <sup>b</sup>	142 ± 2
composition <sup>a</sup>	silica gel, trimethylsilated

<sup>a</sup>As reported by the supplier. <sup>b</sup>Measured in this study.

**Received:** September 26, 2013

**Revised:** November 26, 2013

**Accepted:** December 4, 2013

**Published:** December 4, 2013

DENTSPLY Prosthetics, York, PA) at temperatures ranging from 300 to 600 °C for a period of 8 h in an air atmosphere. As a matter of convention, the resultant samples were named “TLD302-XXX”, where “XXX” indicates the temperature at which heat treatment was performed in degrees Celsius.

**Equilibrium Adsorption Experiments.** Alcohol solutions were prepared using sterile deionized water at a range of initial concentrations typical of alcohol fermentations. Equilibrium adsorption experiments were performed in sterile, 17 mL glass Hungate tubes (Bellco Glass, Vineland, NJ) containing 250 mg of aerogel sample and the remainder (15 mL) aqueous alcohol solution. Tubes were completely filled to leave no headspace, promoting maximal contact between aerogel and liquid. Sealed tubes were used to allow the headspace gas to be completely vented through a needle as the aqueous solution was introduced via a second needle and syringe. In this way the samples were not pressurized. Samples were equilibrated while being agitated at 150 rpm on an orbital shaker at 30 °C for 24 h. Preliminary analyses showed that samples were routinely equilibrated to >95% within about 6 h (data not shown). The specific loading of alcohol adsorbed to aerogel at equilibrium ( $q_e$ ) was determined by the following mass balance relationship:

$$q_e = (C_{aq,0} - C_{aq,e})V_{aq}/m \quad (1)$$

where  $C_{aq,0}$  and  $C_{aq,e}$  are initial and equilibrated aqueous alcohol concentrations, respectively, and  $V_{aq}$  is aqueous phase volume;  $m$  is mass of aerogel. All adsorption experiments were performed in triplicate.

**Equilibrium Adsorption Modeling.** Adsorption equilibrium data were best fit by the Freundlich adsorption isotherm model:

$$q_e = K_F C_{aq,e}^{1/n} \quad (2)$$

where  $K_F$  and  $n$  are the Freundlich adsorption constant and exponent, respectively. Model parameter estimates were obtained from experimental data via nonlinear least-squares regression using the intrinsic MATLAB function *nlinfit*. While multiple adsorption models were initially evaluated,<sup>29</sup> the Freundlich model provided the lowest sum of squared errors (SSE). This finding was consistent with prior works using the same series of alcohol solutes and hydrophobic polymer adsorbents.<sup>30</sup>

**Strains, Media, Culture Conditions, and Bioreactor Operation.** *Clostridium acetobutylicum* ATCC 824 was purchased from the American Type Culture Collection (ATCC; Manassas, VA) and routinely cultured at 37 °C in prereduced reinforced clostridial medium (RCM; BD Difco, Franklin Lakes, NJ). Fermentations were performed using clostridial reactor media (CRM), as prepared according to Mermelstein, et al.,<sup>31</sup> in a 2 L Biostat A Plus bioreactor (Sartorius Stedim Biotech, Bohemia, NY), with BioPAT MFCS/DA 3.0 software used for control and data acquisition. Oxyferm FDA225 and Easyferm Plus K8 200 probes (Hamilton, Reno, NV), were used to monitor dissolved oxygen (DO) and pH, respectively. Glucose-free CRM broth was adjusted initially to a pH of 5.5 in the bioreactor and autoclaved. A concentrated glucose solution (140 g/L) was autoclaved separately and then added to the bioreactor. The 1% (v/v) inoculum was prepared in RCM, as above. Fermentations were performed at a constant temperature of 37 °C, with agitation at 300 rpm, continuous sparging of UHP nitrogen gas

to maintain anaerobic conditions, and Antifoam 204 (Sigma, St. Louis, MO) addition, as needed. Adjustment of pH was performed by automated addition of 5 M  $\text{NH}_4\text{OH}$  or 1 M HCl, as appropriate. After the fermentation, cells were removed from the final broth via microfiltration using a Pellicon XL tangential flow filter (Millipore, Billerica, MA). Under these conditions, *n*-butanol in the fermentation broth reached a final concentration of about 12 g/L (or 162 mM), as determined by high-performance liquid chromatography (HPLC). The clarified broth was then used in batch adsorption studies with TLD302-330, as described above for model alcohol–water solutions, with butanol concentrations in the broth following adsorption also determined by HPLC.

**Analytical Methods.** Aqueous alcohol concentrations were measured via HPLC (1100 series, Agilent, Santa Clara, CA). Separation was achieved on a ZORBAX Eclipse XDB-C18 column (Agilent, Santa Clara, CA) operated at a constant temperature of 50 °C. Filtered and degassed deionized water was used as the mobile phase at a constant flow rate of 1.0 mL/min. Analytes were detected using a refractive index detector operated at 35 °C, and concentrations were determined using external standards.

Contact angle ( $\Theta$ ) measurements of sessile droplets of aqueous alcohol solutions on aerogel surfaces were performed using an EasyDrop (DSA20B, Hamburg, Germany). Aerogel particles were first pressed into disks (diameter of 2.3 cm and thickness of 0.3 cm) to provide a flat surface upon which the sessile droplet could rest as well as a constant baseline for measurements. Disks were formed using a Carver high-pressure press (Model 3925, Wabash, IN) operated at 20,000 psi for 1 min. Contact angles were determined as the angle formed between the droplet–solid interface and the droplet–air interface, providing surface wetting angles between 0 and 90° and nonsurface wetting angles between 90 and 180°. Measurements were repeated four times to ensure reproducibility and to provide an assessment of experimental error. Surface tension ( $\sigma$ ) of aqueous alcohol solutions was measured utilizing a tensiometer (Attension Sigma 700, Västra Frölunda, Sweden) employing a platinum Du Noüy ring. In all cases, measurements were repeated at least four times to ensure reproducibility and to provide an assessment of experimental error.

Elemental analysis was performed to determine the carbon and hydrogen content of aerogels using a Perkin-Elmer 2400 Elemental Analyzer. Samples were loaded into capsules in 3–4 mg increments. The combustion temperature set point was 924 °C and the reduction temperature was 624 °C. Aerogel samples were prepared for FTIR analysis by first being crushed using a mortar and pestle before being loaded onto a disposable KBr transmission FTIR card. Cards were placed into the Bruker IR Scope II (Billerica, MA) equipped with a wide-band MCT detector with a Globar source and a 66 V/S chassis with a KBr beam splitter and wide-band MCT bench detector in transmission mode. All data was obtained by averaging of 32 scans that ranged from wavenumbers of 500 to 8000.

## ■ RESULTS AND DISCUSSION

The equilibrium adsorption behavior of ethanol, *n*-propanol, *n*-butanol, and *n*-pentanol from dilute solutions in water on unmodified TLD302 were elucidated and are compared in Figure 1. The respective Freundlich isotherm model predictions for each alcohol are also compared, with the resultant “best-fit” model parameter estimates for each alcohol being summarized

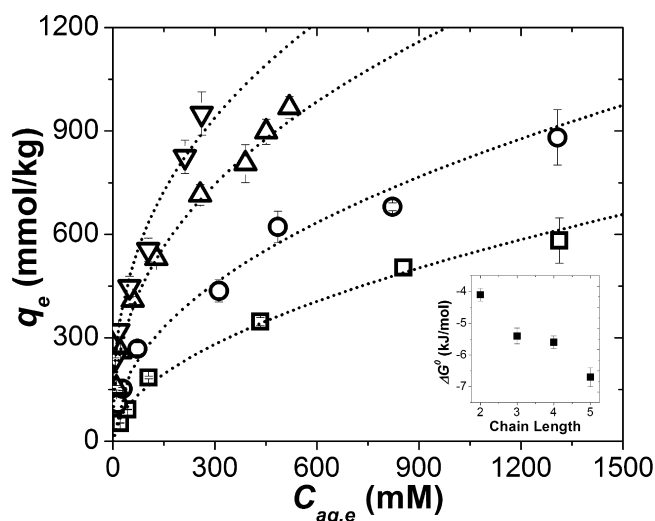


**Figure 1.** Experimental adsorption isotherms of ethanol ( $\square$ ), *n*-propanol ( $\circ$ ), *n*-butanol ( $\triangle$ ), and *n*-pentanol ( $\nabla$ ) upon TLD302 from dilute solutions in water. Freundlich isotherm model predictions for each alcohol are shown as dotted lines. Inset shows the predicted Gibbs free energy changes of alcohol adsorption on TLD302 as a function of chain length ( $\blacksquare$ ). Experimental errors are shown at one standard deviation.

in Table 2. Both  $K_F$  and  $n$  were positively correlated with the alkyl chain length for each alcohol; for example,  $K_F$  increases

**Table 2.** Freundlich Isotherm “Best-Fit” Parameter Estimates for Ethanol, *n*-Propanol, *n*-Butanol, and *n*-Pentanol on TLD302 Obtained under Dilute Conditions<sup>a</sup>

alcohol	$\log K_{O/W}$	$K_F$ (mmol/kg)	$n$
ethanol	−0.26	$10 \pm 3$	$1.67 \pm 0.14$
<i>n</i> -propanol	0.07	$34 \pm 4$	$2.18 \pm 0.10$
<i>n</i> -butanol	0.80	$62 \pm 6$	$2.27 \pm 0.10$
<i>n</i> -pentanol	1.13	$112 \pm 12$	$2.71 \pm 0.19$

<sup>a</sup>Error associated with all parameter estimates are reported at one standard deviation.

with an increase in carbon chain length. Perhaps more appropriately, however,  $K_F$  and  $n$  were positively correlated with the alcohols’  $\log K_{O/W}$  values (log of the octanol–water partitioning coefficient), which provide a measure of relative hydrophobicity. This latter correlation supports a mechanism of hydrophobic adsorption (i.e., van der Waals interactions) wherein the more hydrophobic solutes (i.e., those with longer chains) are adsorbed most strongly and to the greatest extent. This trend is notably consistent with that of prior works wherein hydrophobic polymeric adsorbents were investigated for the separation of the same 2- to 5-carbon alcohols from water.<sup>17</sup> Furthermore, similar trends were also recently reported for the adsorption of 2- to 6-carbon diols and triols on zeolites of various pore sizes (including FER, MWW, MFI, BEA, MOR, and FAU) and on ordered mesoporous materials (including MCM-36, 3Dom-MFI, and SBA-15).<sup>32</sup> Relative adsorption strengths, meanwhile, were compared by estimating the Gibbs free energy change of adsorption ( $\Delta G^0$ ) for each alcohol. With adsorption isotherms represented by the Freundlich model,  $\Delta G^0$  can be estimated as<sup>33,34</sup>

$$\Delta G^0 = -nRT \quad (3)$$

where  $R$  is the universal gas constant,  $T$  the temperature, and  $n$  the Freundlich adsorption exponent from eq 2. Predicted  $\Delta G^0$  values are compared in the inset of Figure 1 as a function of alcohol chain length, wherein an inverse, linear correlation is clearly observed. Negative  $\Delta G^0$  values are consistent with the fact that alcohol adsorption on aerogels is a spontaneous process. More importantly, all  $\Delta G^0$  estimates are consistent with the proposed mechanism of physical adsorption, as values of about  $-20$  kJ/mol and below are typically consistent with “weak interactions”<sup>34,35</sup> (e.g., van der Waals interactions).  $\Delta G^0$  values exceeding about  $-40$  kJ/mol, on the other hand, would result because of “strong interactions”, such as chemisorption.<sup>36</sup> As a point of comparison,  $\Delta G^0$  of ethanol and *n*-butanol adsorption from water on the hydrophobic, macroporous poly(styrene-co-divinylbenzene) adsorbent Dowex Optipore L-493 at  $30^\circ\text{C}$  were previously estimated as  $-3.1$  and  $-5.3$  kJ/mol, respectively. Additionally, the  $\Delta G^0$  of *n*-butanol adsorption from water on high silica MEL type zeolite at  $30^\circ\text{C}$ , for example, was estimated to be between  $-11.8$  to  $-12.8$  kJ/mol.<sup>37</sup> Most importantly, this implies that the adsorption can be readily reversed, a necessity for adsorbent regeneration and ultimate recovery of the separated alcohol.

The adsorption behavior of all four alcohols on TLD302 was next characterized in concentrated water solutions, the results of which are compared in Figure 2 (note: to maintain single

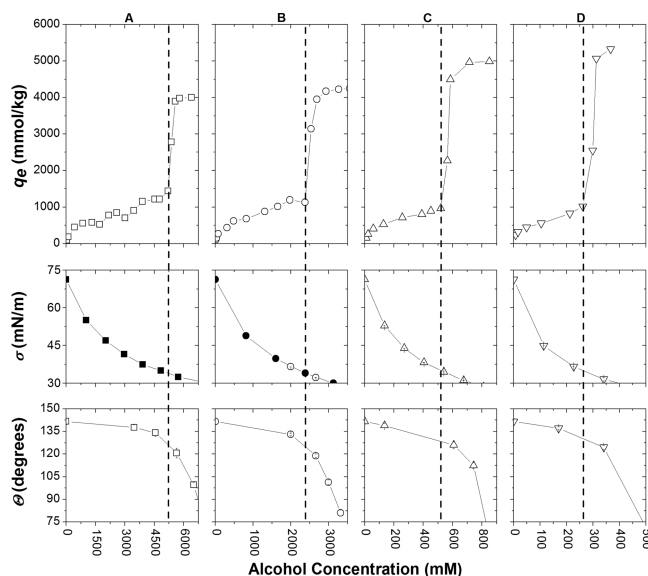


**Figure 2.** Experimental adsorption isotherms of ethanol (A,  $\square$ ), *n*-propanol (B,  $\circ$ ), *n*-butanol (C,  $\triangle$ ), and *n*-pentanol (D,  $\nabla$ ) upon TLD302 from concentrated solutions in water (upper panels). Interpreted “critical aqueous concentrations” ( $C_{aq,crit}$ ) are indicated by dashed vertical lines. Also shown are surface tension ( $\sigma$ ; middle panels) and contact angle on TLD302 ( $\theta$ ; lower panels) measured as a function of concentration for all four alcohols. Open shapes are data from this study while solid shapes are literature values from Vazquez et al.<sup>38</sup> Experimental errors are shown at one standard deviation.

liquid phases, focal concentration ranges were varied with respect to the solubility limit of each alcohol). As seen in Figure 2, a so-called “critical aqueous concentration” ( $C_{aq,crit}$ ) was found to emerge along the equilibrium isotherm of each alcohol above which the specific loading capacity ( $q_e$ ) increased significantly in response to only a small increases in equilibrated alcohol concentration. In the case of *n*-butanol, for example,



while  $q_e$  approached about 970 mmol/kg as  $C_{aq,e}$  was increased from 0 to 520 mM, a >5-fold jump in  $q_e$  (to ~5000 mmol/kg) occurred as  $C_{aq,e}$  was then further increased from 520 to just 720 mM.  $C_{aq,crit}$  values were found to be unique to each alcohol, existing at approximately 5200, 2400, 520, and 260 mM for ethanol, *n*-propanol, *n*-butanol, and *n*-pentanol, respectively, implying an inverse correlation with chain length and thus hydrophobicity of the alcohol solute. It is further interesting to note that specific loading capacities of all four alcohols were nearly identical at their respective  $C_{aq,crit}$  values, ranging between just 1100 to 1400 mmol/kg (Figure 2).

In addition, qualitative changes in adsorbent behavior were also noted as alcohol solution concentrations approached and ultimately surpassed their respective  $C_{aq,crit}$  values. For instance, below  $C_{aq,crit}$  TLD302 particles accumulated just below the aqueous surface at the top of the sample tube, with said buoyancy resulting from the presence of air within the pores. However, as aqueous alcohol concentrations were increased, approaching and ultimately surpassing  $C_{aq,crit}$ , rapid displacement of air from TLD302's pores was observed, as accompanied by the influx of aqueous solution. This was then immediately followed by the sinking of TLD302 particles and their accumulation at the bottom of the sample tube. After this process of "pore intrusion", solutes gained access to those surface adsorption sites existing within TLD302's extensive intraparticle pore structure, leading to further adsorption and greatly enhanced specific loadings as a result (Figure 2).

The above findings collectively suggested that occurrences of pore intrusion and its resultant benefit to adsorption capacity were influenced by changes in solution properties, arising herein as a function of both alcohol concentration and chain length. Accordingly, subsequent investigations further revealed that at each respective  $C_{aq,crit}$  value, all four alcohol solutions also displayed similar surface tensions and wetting characteristics upon TLD302 (noting that the observed trend for *n*-propanol agrees well with that of prior works<sup>38</sup>). More specifically, regardless of the alcohol chain length, at  $C_{aq,crit}$  each alcohol solution (a) possessed a surface tension that was about 31–36 mN/m and (b) demonstrated a minimum contact angle of ~125° on TLD302 (Figure 2). In contrast, pure water was measured to have a surface tension of 72 mN/m and was found to wet TLD302 at a contact angle of ~142° (which is consistent with prior reports of ~135–155° contact angles for sessile water droplets on hydrophobic aerogels<sup>2</sup>). The observation that effective surface wetting is an essential prerequisite to pore intrusion suggests that a minimum surface energy barrier exists between the solution and aerogel phases, one that is overcome only when the solution becomes sufficiently hydrophobic, as satisfied either extrinsically or intrinsically (i.e., by increasing alcohol concentration or by increasing the alcohol chain length, respectively).

In light of this finding, it was postulated that improved aerogel surface wetting could alternatively be achieved by altering the surface chemistry of the aerogel itself, rendering it as less hydrophobic. In prior works it has been shown that heat treatment of methyl functionalized silica aerogel at temperatures ranging from 350 to 500 °C differentially reduced its hydrophobicity because of the partial to complete oxidation of surface  $-\text{CH}_3$  groups.<sup>39</sup> In the present application, it was anticipated that partial oxidation of TLD302's  $-\text{C}(\text{CH}_3)_3$  surface functional groups would reduce its hydrophobicity to accommodate pore intrusion under more dilute conditions, rendering the aerogel as a more effective adsorbent across a

wider range of concentrations. However, as doing so would also coincidentally reduce the net strength of the hydrophobic interactions responsible for adsorption, a decrease in overall adsorption capacity was likewise expected as a result. Thus, it was further hypothesized that an optimum state of partial surface oxidation would exist, wherein facile pore intrusion and high adsorption capacities would be appropriately balanced.

As described above, oxidation of TLD302's surface groups was accomplished by heat treatment of aerogel samples in an air atmosphere at temperatures ranging from 300 to 600 °C for a period of 8 h. As seen in Table 3, this process resulted in the

**Table 3. Carbon and Hydrogen Content of Aerogel Samples Determined As a Function of the Temperature at Which Heat Treatment Was Performed<sup>a</sup>**

aerogel	carbon (wt%)	hydrogen (wt%)
TLD302	10.54 ± 0.01	3.09 ± 0.01
TLD302-315	9.84 ± 0.01	2.83 ± 0.04
TLD302-325	9.71 ± 0.02	2.73 ± 0.01
TLD302-330	9.57 ± 0.11	2.75 ± 0.02
TLD302-400	2.68 ± 0.01	0.62 ± 0.01

<sup>a</sup>Error associated with all parameter estimates are reported at one standard deviation.

reduction of both carbon and hydrogen content in aerogel samples, suggesting a loss of surface methyl groups. For instance, whereas between temperatures of 315 and 330 °C, the carbon content of aerogel samples initially underwent a gradual decrease in a linear manner (at a rate of  $0.013 \pm 0.001$  wt % carbon per °C;  $R^2 = 0.996$ ), samples treated at 400 °C were then found to be greatly reduced in carbon content, containing just  $2.68 \pm 0.11$  wt % carbon (with insignificant additional losses up to 600 °C; data not shown). Furthermore, FTIR analysis showed that as samples aerogel samples were heated to 400 °C, absorption peaks at 2964, 1256, and 846  $\text{cm}^{-1}$  corresponding to  $-\text{CH}_3$  terminal groups<sup>39</sup> were decreased, whereas a broad peak spanning between 3200 and 3600  $\text{cm}^{-1}$  corresponding to  $-\text{OH}$  groups coincidentally emerged (Figure 3). These results suggested that the heat treatment process was successful at reducing the content of nonpolar terminal groups on TLD302's surface while increasing the concentration of polar terminal groups, factors that would both effectively reduce the aerogel surface hydrophobicity.

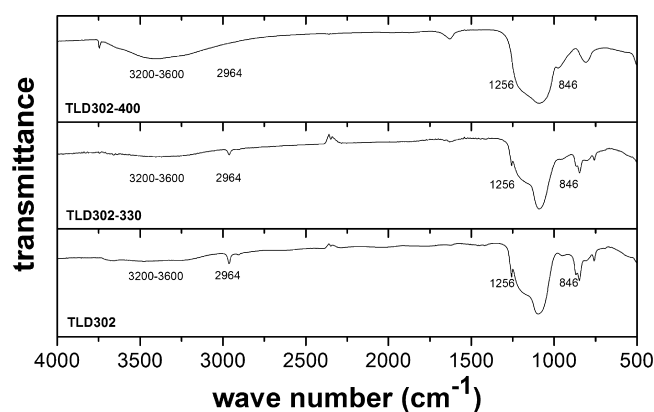


**Figure 3.** Infrared spectra of aerogel samples TLD302, TLD302-330, and TLD302-400.

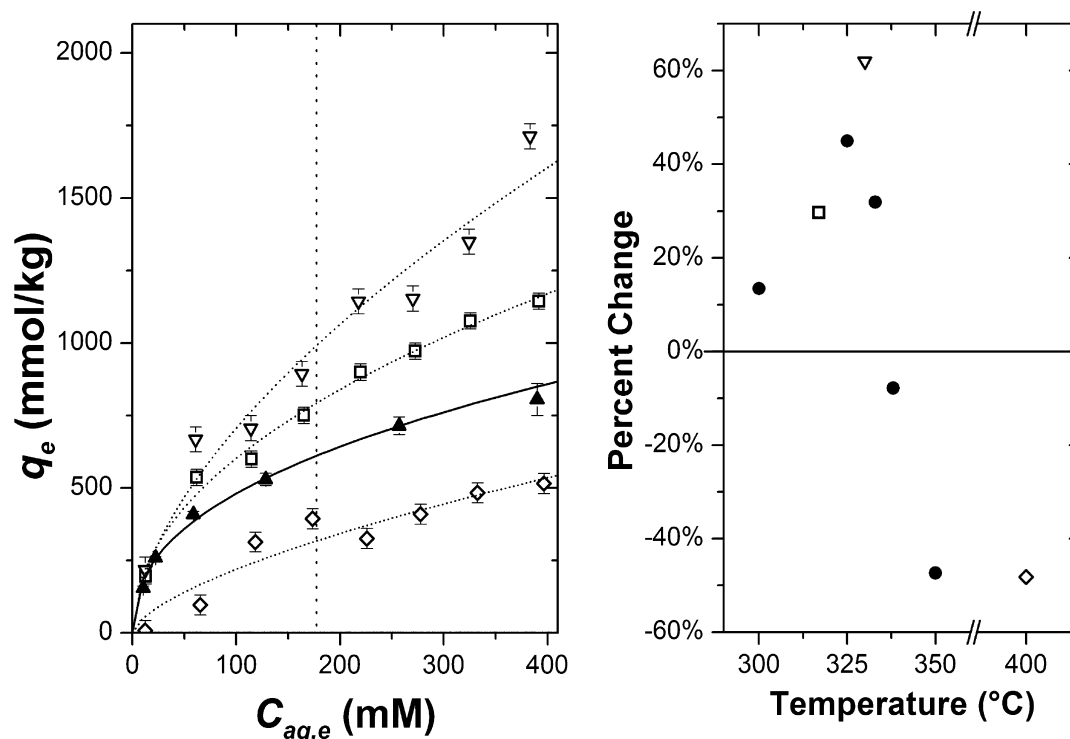


**Figure 4.** Left panel: experimental and best-fit isotherm model predictions of *n*-butanol adsorption on TLD302 (▲, solid line), TLD302-317 (□, dashed line), TLD302-330 (▽, dashed line), TLD302-400 (◇, dashed line). Dashed vertical line at an equilibrated aqueous concentration of 175 mM represents a cross-section of isotherm values selected for further comparison in the right panel. Right panel: percent change (relative to TLD302) in predicted *n*-butanol-specific loading on TLD302-derived aerogels (●), plotted as a function of the temperature at which heat treatment was performed. Experimental errors are shown at one standard deviation.

The resultant, TLD302-derived materials were subsequently characterized with respect to their equilibrium adsorption behavior, in this case, however, for just *n*-butanol. The equilibrium isotherms are compared in Figure 4, whereas their resultant best-fit Freundlich isotherm model parameters are compared in Table 4 (note: the isotherms of a limited

**Table 4. Freundlich Isotherm “Best-Fit” Parameter Estimates for *n*-Butanol on Select TLD302-Derived Aerogels Obtained under Dilute Conditions<sup>a</sup>**

aerogel	$K_F$ (mmol/kg)	$n$
TLD302	$62 \pm 6$	$2.27 \pm 0.10$
TLD302-317	$66 \pm 14$	$2.09 \pm 0.28$
TLD302-330	$46 \pm 8$	$1.69 \pm 0.51$
TLD302-400	$11 \pm 4$	$1.55 \pm 0.78$

<sup>a</sup>Error associated with all parameter estimates are reported at one standard deviation.

selection of all TLD302-derived materials are shown and compared for clarity). Relative to TLD302 as control, it can be seen that samples prepared at temperatures of up to 333 °C (i.e., TLD302-300, -317, -325, -330, and -333) were each enhanced in their *n*-butanol adsorption ability whereas those prepared at 338 °C and above (i.e., TLD302-338, -350, and -400) all performed worse. An optimum was in fact observed to occur at 330 °C, with the equilibrium adsorption capacity of TLD302-330 being higher than TLD302 at all equilibrated *n*-butanol concentrations, and specifically up to 60% higher at 175 mM (the would be inhibitory limit in a fermentation). Note that the carbon content of TLD302-330 was found to be

$9.57 \pm 0.11$  wt % (Table 3), a  $9 \pm 1\%$  reduction relative to TLD302.

Whereas the adsorption performance of TLD302-330 was significantly enhanced over that of TLD302, as seen in Figure 5, further room for improvement still exists when aerogels are compared against other, more well-characterized butanol

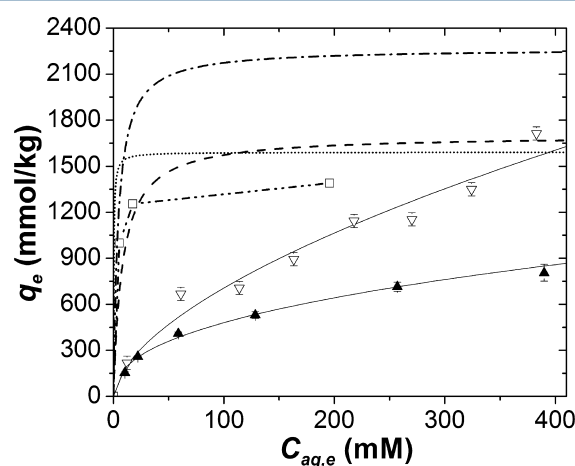


**Figure 5.** Comparison of *n*-butanol adsorption isotherms upon TLD302 (▲) and TLD302-330 (▽) and their respective Freundlich isotherm model fits (solid lines) with literature values reported for hydrophobic, silica zeolite adsorbents, including those from Milestone and Bibby,<sup>43</sup> *n*-butanol/silicalite-1 (□ with dash-dot-dot line), and Oudshoorn,<sup>44</sup> *n*-butanol/Zeolyst CBV901 (dash-dot line), *n*-butanol/Zeolyst CBV9811C-300 (dashed line), and *n*-butanol/Zeolyst CBV28014 (dotted line).

adsorbents.<sup>26,40–42</sup> Among these, high silica, hydrophobic zeolites are most similar to aerogels in chemistry and thus provide for the most fair comparison. Whereas the gap has been narrowed with respect to adsorption capacity, the apparent *n*-butanol adsorption affinity of materials such as silicalite-1<sup>43</sup> and Zeolyst<sup>44</sup> remain much greater. Further improvements in the affinity of aerogels for *n*-butanol adsorption will likely come from de novo synthesis of materials with specifically tuned hydrophobicity achieved through the incorporation of novel surface functional groups.

Lastly, to be effective in applications in which the alcohols to be separated are biofuels (ethanol and *n*-butanol, for example), adsorbents should perform well not only in model solutions but also, and most importantly, when employed in fermentation broths. However, complex fermentation broths contain numerous inorganic and organic species (e.g., media components and fermentation byproducts) that can act as foulants, competitively inhibiting the uptake of the target molecule through their coadsorption. A preliminary appraisal of the robustness of TLD302-330 under such conditions was performed by comparing its equilibrium adsorption for *n*-butanol from actual fermentation broths with that of model solutions. As seen in Figure 6, the adsorption behavior of *n*-

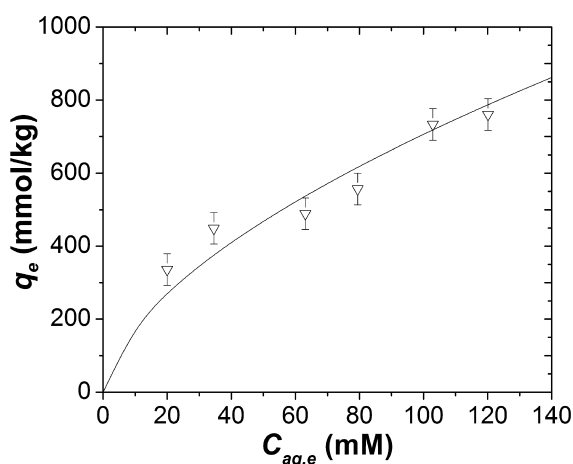


**Figure 6.** Experimental adsorption isotherm of *n*-butanol from clarified fermentation broths of *C. acetobutylicum* ATCC 824 on TLD302-330 ( $\nabla$ ). The Freundlich isotherm model prediction based on best-fit parameters obtained from model solutions (i.e., butanol:water) is also shown for comparison. Experimental errors are shown at one standard deviation.

butanol on TLD302-330 is resilient to the presence of other components found in a *C. acetobutylicum* ATCC 824 fermentation broth. While promising, more extensive and longer-term characterizations are certainly needed before hydrophobic aerogels should be deployed as adsorbents for biofuel alcohol recovery.

## CONCLUSIONS

While bulk transport limitations reduced the achievable alcohol adsorption by TLD302 under dilute conditions, improved surface wetting at higher concentrations enabled pore intrusion and greatly improved separation. Tuning of aerogel surface properties was ultimately found to be an effective strategy for improving separation across a wider range of concentrations and for less hydrophobic solutes. Hydrophobic aerogels are a promising class of adsorbent materials for the separation of

alcohols, including biofuels, from aqueous solutions. Further tuning of surface properties via appropriate functionalization, however, will be required before they are able to achieve their full potential.

## AUTHOR INFORMATION

### Corresponding Author

\*Tel.: (480) 965-4113. Fax: (480) 727-9321. E-mail: David.R.Nielsen@asu.edu.

### Notes

The authors declare no competing financial interest.

## ACKNOWLEDGMENTS

M.T.W. and T.J.L. were supported by financial assistance from both the U.S. Department of Energy, Office of ARPA-E (Award DE-AR0000011) and Arizona State University. K.S. was supported by financial assistance from the National Science Foundation (Award CBET-1067684). We thank Dr. Lenore Dai and Sriya Sanyal (ASU) for assistance with surface tension measurements, Mr. Michael Dodson (ASU) for assistance with contact angle measurements, and Dr. Dhaval Doshi and Mr. A. J. DuPlessis (Cabot Corporation) for supplying the Nanogel used in the experiments. We wish to thank Dr. Wei Yuan for many helpful discussions.

## REFERENCES

- (1) Tabata, M.; Adachi, I.; Ishii, Y.; Kawai, H.; Sumiyoshi, T.; Yokogawa, H. Development of transparent silica aerogel over a wide range of densities. *Nucl. Instrum. Methods Phys. Res., Sect. A* **2010**, *623* (1), 339–341.
- (2) Wagh, P. B.; Ingale, S. V.; Gupta, S. C. Comparison of hydrophobicity studies of silica aerogels using contact angle measurements with water drop method and adsorbed water content measurements made by Karl Fischer's titration method. *J. Sol–Gel Sci. Tech.* **2010**, *55* (1), 73–78.
- (3) Reynolds, J. G.; Coronado, P. R.; Hrubesh, L. W. Hydrophobic aerogels for oil-spill cleanup—Intrinsic absorbing properties. *Energy Sources* **2001**, *23* (9), 831–843.
- (4) Standeker, S.; Novak, Z.; Knez, Z. Adsorption of toxic organic compounds from water with hydrophobic silica aerogels. *J. Colloid Interface Sci.* **2007**, *310* (2), 362–368.
- (5) Liu, H. J.; Sha, W.; Cooper, A. T.; Fan, M. H. Preparation and characterization of a novel silica aerogel as adsorbent for toxic organic compounds. *Colloids Surf., A* **2009**, *347* (1–3), 38–44.
- (6) Gorle, B. S. K.; Smirnova, I.; McHugh, M. A. Adsorption and thermal release of highly volatile compounds in silica aerogels. *J. Supercrit. Fluids* **2009**, *48* (1), 85–92.
- (7) Wang, D.; McLaughlin, E.; Lin, Y. S.; Pfeffer, R. Aqueous phase adsorption of toluene in a packed and fluidized bed of hydrophobic aerogels. *Chem. Eng. J.* **2011**, *168* (3), 1201–1208.
- (8) Reynolds, J. G.; Coronado, P. R.; Hrubesh, L. W. Hydrophobic aerogels for oil-spill clean up – synthesis and characterization. *J. Non-Cryst. Solids* **2001**, *292* (1–3), 127–137.
- (9) Aravind, P.; Soraru, G. High surface area methyltriethoxysilane-derived aerogels by ambient pressure drying. *J. Porous Mater.* **2011**, *18* (2), 159–165.
- (10) Gurav, J.; Rao, A.; Nadargi, D.; Park, H. Ambient pressure dried TEOS-based silica aerogels: Good absorbents of organic liquids. *J. Mater. Sci.* **2010**, *45* (2), 503–510.
- (11) Cui, S.; Liu, X.; Liu, Y.; Shen, X.; Lin, B.; Han, G.; Wu, Z. Adsorption properties of nitrobenzene in wastewater with silica aerogels. *Sci. China: Technol. Sci.* **2010**, *53* (9), 2367–2371.
- (12) Love, A.; Hanna, M.; Reynolds, J. Engineering Surface Functional Groups on Silica Aerogel for Enhanced Cleanup of Organics from Produced Water. *Sep. Sci. Technol.* **2005**, *40* (1–3), 311–320.

- (13) Kaminski, W.; Tomczak, E.; Gorak, A. Biobutanol - Production and Purification Methods. *Ecol. Chem. Eng. S* **2011**, *18* (1), 31–37.
- (14) Luyben, W. L. Control of the Heterogeneous Azeotropic *n*-Butanol/Water Distillation System. *Energy Fuels* **2008**, *22* (6), 4249–4258.
- (15) Ladisch, M. R.; Dyck, K. Dehydration of Ethanol: New Approach Gives Positive Energy-Balance. *Science* **1979**, *205* (4409), 898–900.
- (16) Nielsen, D. R.; Prather, K. J. In Situ Product Recovery of *n*-Butanol Using Polymeric Resins. *Biotechnol. Bioeng.* **2009**, *102* (3), 811–821.
- (17) Nielsen, D. R.; Amarasiriwardena, G. S.; Prather, K. L. J. Predicting the adsorption of second generation biofuels by polymeric resins with applications for in situ product recovery (ISPR). *Bioresour. Technol.* **2010**, *101* (8), 2762–2769.
- (18) Straathof, A. J. J.; Oudshoorn, A.; van der Wielen, L. A. M. Adsorption equilibria of bio-based butanol solutions using zeolite. *Biochem. Eng. J.* **2009**, *48* (1), 99–103.
- (19) Silvestre-Albero, J.; Silvestre-Albero, A.; Sepulveda-Escribano, A.; Rodriguez-Reinoso, F. Ethanol removal using activated carbon: Effect of porous structure and surface chemistry. *Microporous Mesoporous Mater.* **2009**, *120* (1–2), 62–68.
- (20) Saravanan, V.; Wijers, D. A.; Ziari, M.; Noordermeer, M. A. Recovery of 1-butanol from aqueous solutions using zeolite ZSM-5 with a high Si/Al ratio; Suitability of a column process for industrial applications. *Biochem. Eng. J.* **2010**, *49* (1), 33–39.
- (21) Huang, Y. W.; Fu, J. W.; Pan, Y.; Huang, X. B.; Tang, X. Z. Pervaporation of ethanol aqueous solution by polyphosphazene membranes: Effect of pendant groups. *Sep. Purif. Technol.* **2009**, *66* (3), 504–509.
- (22) Ma, Y.; Wang, J. H.; Tsuru, T. Pervaporation of water/ethanol mixtures through microporous silica membranes. *Sep. Purif. Technol.* **2009**, *66* (3), 479–485.
- (23) Inokuma, K.; Liao, J. C.; Okamoto, M.; Hanai, T. Improvement of isopropanol production by metabolically engineered *Escherichia coli* using gas stripping. *J. Biosci. Bioeng.* **2010**, *110* (6), 696–701.
- (24) Ezeji, T. C.; Qureshi, N.; Blaschek, H. P. Production of acetone, butanol and ethanol by *Clostridium beijerinckii* BA101 and in situ recovery by gas stripping. *World J. Microbiol. Biotechnol.* **2003**, *19* (6), 595–603.
- (25) Vane, L. M. Separation technologies for the recovery and dehydration of alcohols from fermentation broths. *Biofuels, Bioprod. Biorefin.* **2008**, *2* (6), 553–588.
- (26) Qureshi, N.; Hughes, S.; Maddox, I. S.; Cotta, M. A. Energy-efficient recovery of butanol from model solutions and fermentation broth by adsorption. *Bioprocess Biosyst. Eng.* **2005**, *27* (4), 215–222.
- (27) Oudshoorn, A.; van der Wielen, L. A. M.; Straathof, A. J. J. Assessment of Options for Selective 1-Butanol Recovery from Aqueous Solution. *Ind. Eng. Chem. Res.* **2009**, *48* (15), 7325–7336.
- (28) Nielsen, D. R.; Amarasiriwardena, G. S.; Prather, K. J. Predicting the Adsorption of Second Generation Biofuels by Polymeric Resins with Applications for In Situ Product Recovery (ISPR). *Bioresour. Technol.* **2009**, *101*, 2762–2769.
- (29) Foo, K. Y.; Hameed, B. H. Insights into the modeling of adsorption isotherm systems. *Chem. Eng. J.* **2012**, *156*, 2–10.
- (30) Nielsen, D. R.; Amarasiriwardena, G. S.; Prather, K. L. Predicting the adsorption of second generation biofuels by polymeric resins with applications for in situ product recovery (ISPR). *Bioresour. Technol.* **2010**, *101* (8), 2762–9.
- (31) Mermelstein, L. D.; Welker, N. E.; Petersen, D. J.; Bennett, G. N.; Papoutsakis, E. T. Genetic and metabolic engineering of *Clostridium acetobutylicum* ATCC 824. *Ann. N. Y. Acad. Sci.* **1994**, *721*, 54–68.
- (32) Mallon, E. E.; Bhan, A.; Tsapatsis, M. Driving Forces for Adsorption of Polyols onto Zeolites from Aqueous Solutions. *J. Phys. Chem. B* **2010**, *114* (5), 1939–1945.
- (33) Huang, H. H.; Zhou, Y.; Huang, K. L.; Liu, S. Q.; Luo, Q.; Xu, M. C. Adsorption behavior, thermodynamics, and mechanism of phenol on polymeric adsorbents with amide group in cyclohexane. *J. Colloid Interface Sci.* **2007**, *316* (1), 10–18.
- (34) Kuo, C. Y.; Wu, C. H.; Wu, J. Y. Adsorption of direct dyes from aqueous solutions by carbon nanotubes: Determination of equilibrium, kinetics and thermodynamics parameters. *J. Colloid Interface Sci.* **2008**, *327* (2), 308–315.
- (35) Ibezim-Ezeani, M. U.; Anusiem, A. C. I. Thermodynamics of the adsorption of palmitate and laurate soaps onto some metal ore surfaces in aqueous media. *Afr. J. Pure Appl. Chem.* **2011**, *5* (9), 272–277.
- (36) Horsfall, M., Jr.; Abia, A. A.; Spiess, A. I. Kinetic studies on the adsorption of Cd<sup>2+</sup>, Cu<sup>2+</sup> and Zn<sup>2+</sup> ions from aqueous solutions by cassava (*Manihot sculenta* Cranz) tuber bark waste. *Bioresour. Technol.* **2006**, *97* (2), 283–91.
- (37) Sharma, P.; Chung, W. J. Synthesis of MEL type zeolite with different kinds of morphology for the recovery of 1-butanol from aqueous solution. *Desalination* **2011**, *275* (1–3), 172–180.
- (38) Vazquez, G.; Alvarez, E.; Navaza, J. M. Surface Tension of Alcohol + Water from 20 to 50 °C. *J. Chem. Eng. Data* **1995**, *40* (3), 611–614.
- (39) Shi, F.; Wang, L. J.; Liu, J. X.; Zeng, M. Effect of heat treatment on silica aerogels prepared via ambient drying. *J. Mater. Sci. Technol. (Shenyang, China)* **2007**, *23* (3), 402–406.
- (40) Bayrak, Y. Application of Langmuir isotherm to saturated fatty acid adsorption. *Microporous Mesoporous Mater.* **2006**, *87* (3), 203–206.
- (41) Sanemasa, I.; Nakahara, M.; Zheng, J. Z. Uptake of alkanes and alcohols by ion-exchange resins in aqueous solution. *Anal. Sci.* **2003**, *19* (6), 949–951.
- (42) Yang, X. P.; Tsai, G. J.; Tsao, G. T. Enhancement of *in situ* adsorption on the acetone-butanol fermentation by *Clostridium acetobutylicum*. *Sep. Technol.* **1994**, *4* (2), 81–92.
- (43) Milestone, N. B.; Bibby, D. M. Concentration of Alcohols by Adsorption on Silicalite. *J. Chem. Technol. Biotechnol.* **1981**, *31* (12), 732–736.
- (44) Oudshoorn, A.; van der Wielen, L. A. M.; Straathof, A. J. J. Adsorption equilibria of bio-based butanol solutions using zeolite. *Biochem. Eng. J.* **2009**, *48* (1), 99–103.